Biofilm 6 (2023) 100159

Contents lists available at ScienceDirect

Biofilm

journal homepage: www.sciencedirect.com/journal/biofilm

Hyperbaric oxygen therapy counteracts *Pseudomonas aeruginosa* biofilm micro-compartment phenomenon in murine thermal wounds

Anne Sofie Laulund [a,*], Franziska Angelika Schwartz [b], Niels Høiby [c], Kim Thomsen [d], Claus Moser [e]

[a] *Department of Clinical Microbiology, Copenhagen University Hospital, Rigshospitalet, Henrik Harpestrengs Vej 4A, 2100, Copenhagen, Denmark*
[b] *Department of Clinical Microbiology, Copenhagen University Hospital, Rigshospitalet, Denmark*
[c] *Department of Clinical Microbiology, Rigshospitalet, Copenhagen University Hospital and Department of Immunology and Microbiology (ISIM), University of Copenhagen, Denmark*
[d] *Department of Clinical Microbiology, Zealand University Hospital, Denmark*
[e] *Department of Clinical Microbiology, Copenhagen University Hospital, Rigshospitalet and Department of Immunology and Microbiology (ISIM), University of Copenhagen, Denmark*

A B S T R A C T

Background: Biofilm antibiotic tolerance is partly explained by the behavior of a biofilm as an independent pharmacokinetic micro-compartment. Hyperbaric oxygen therapy has been shown to potentiate antibiotic effects in biofilms. The present study investigates the effect of hyperbaric oxygen therapy (HBOT) on the biofilm micro-pharmacokinetic/pharmacodynamic behavior of tobramycin in an animal biofilm model.

Methods: Full-thickness necroses were created mid-scapular on mice by means of a thermal lesion. After four days, three 16 h seaweed alginate biofilm beads containing *Pseudomonas aeruginosa* PAO1 were inserted under the necrosis, and three beads were inserted under the adjacent non-affected skin. The mice were randomized to three groups I) HBOT for 1.5 h at 2.8 atm and 0.8 mg tobramycin/mouse subcutaneously; II) Tobramycin as monotherapy, same dose; III) Saline control group. Half the number of mice from group 1 and 2 were sacrificed, and beads were recovered *in toto* after 3 h and the other half and the placebo mice were sacrificed and beads collected after 4.5 h.

Results: Lower CFUs were seen in the burned group receiving HBOT at 3 and 4.5 h compared to beads in the atmospheric environment ($p = 0.043$ and $p = 0.0089$). At 3 h, no CFU difference was observed in the non-burned skin (HBOT vs atmospheric). At 4.5 h, CFU in the non-burned skin had lower CFUs in the group receiving HBOT compared to the corresponding atmospheric group ($p = 0.02$). CFU was higher in the burned skin than in the non-burned skin at 3 h when HBOT was applied ($p = 0.04$), effect faded out at 4.5 h.

At both time points, the tobramycin content in the beads under burned skin were higher in the HBOT group than in the atmospheric groups ($p = 0.031$ and $p = 0.0078$). Only at 4.5 h a higher tobramycin content was seen in the beads under the HBOT-treated burned skin than the beads under the corresponding non-burned skin ($p = 0.006$).

Conclusion: HBOT, as an anti-biofilm adjuvant treatment of chronic wounds, counteracts biofilm pharmacokinetic micro-compartmentalization through increased available tobramycin and augmented bacterial killing.

1. Introduction

Biofilms reside in approximately 80% of chronic wounds and represent a treatment challenge [1]. It was previously demonstrated *in vitro* and *in vivo* that biofilm behaves as an independent third pharmacological microcompartment [2–4]. Blood and wound tissue is considered the pharmacokinetic system's first and second compartments when an antibiotic is administered systemically, whereas the distinct biofilm with matrix, can behave as a third antibiotic pharmacokinetic micro-compartment [4,5].

The ability of bacterial cells in a biofilm to endure in the presence of antimicrobial treatments without genetic alterations is referred to as tolerance. Resistance entails acquiring genetic alterations or mutations that impart a particular mechanism to avoid the effects of antibiotics actively. Unlike tolerance, resistance is typically specific to a particular antibiotic or class of antibiotics [6].

Tolerant cells display reversible phenotypic changes within the biofilm by transition into a less metabolically active or dormant state, referred to as the persister phenotype. The dormant persister phenonemon is argued to be an oversimplification of a complex persistence mechanism [7]. A general consensus is that the tolerance phenonemon frequently results in repeated relapses of infections. Although tolerant

* Corresponding author.
E-mail address: annesofielaulund@gmail.com (A.S. Laulund).

https://doi.org/10.1016/j.bioflm.2023.100159
Received 14 August 2023; Received in revised form 20 September 2023; Accepted 24 September 2023
Available online 26 September 2023

cells show less sensitivity to antibiotics, they can still be eradicated when exposed to higher concentrations, for longer periods, or in combination with adjuvant treatments [8].

The recalcitrance of a biofilm toward antibiotics is considered multifactorial [9]. Biofilms produce a complex microenvironment that differs locally in terms of available nutrients, the amount of oxygen present, the pH, and the diffusion barriers. These chemical and spatial heterogeneities influence the distribution and penetration of antimicrobial drugs within the biofilm. As a result of the extracellular polymeric substance (EPS) or matrix restriction on drug diffusion, concentration gradients between biofilm levels are created [10]. The deeper layers, where persistent bacteria remain, may not receive appropriate therapeutic antibiotic concentrations. Additionally, a decreased metabolic activity inside biofilms might extend medication exposure by slowing down the processes of drug absorption, distribution, and elimination and potentially changing the pharmacokinetic characteristics of antimicrobial drugs.

An additional key factor for the insufficient treatment of recalcitrant wound biofilm is the oxygen deprivation in the wound bed [11]. The cells of the wound survive mainly on anaerobic metabolism and stimulated hypoxia-inducible factors (HIF) up-regulating vasodilation [12,13]. In a chronic wound, these actions are insufficient to meet the O_2 demand of the healing process. An increased O_2 concentration regulates the ischemia-reperfusion-induced leukocyte influx, stimulates neutrophil bactericidal activity, fibroblast proliferation and angiogenesis, and is believed to hinder bacterial growth [14–16].

Hypoxia also contributes to the internal anoxic biofilm conditions differing approximately 50 μm from the biofilm surface [17]. O_2 limitation is estimated to be responsible for 69% of the *P. aeruginosa* biofilms tolerance of tobramycin [2]. The transport of tobramycin across the membrane is an O_2-dependent process, further complicating the matter [3]. By introducing an increased atmospheric pressure at 2.8 bar and 100% oxygen as an external component, bacteria may be re-sensitized to tobramycin killing caused by ATP production and dependent uptake of tobramycin. This antibiotic-potentiating effect can be achieved in a hyperbaric oxygen (HBOT) chamber.

To further illuminate the beneficial effect of HBOT in the context of distinct biofilm compartments of the infected wound, we investigated whether HBOT could improve the tobramycin uptake in the biofilm and decrease the bacterial load in an *in vivo* mouse *P. aeruginosa* biofilm thermal wound model.

2. Method

2.1. In vivo model

The *in vivo* model is approved by the Danish animal welfare legislation (Permission nr. 2020-15-0201-00535). Female 11-week-old BALB/c mice from Janvier Labs (Rte. du Genest, 53940 Le Genest-Saint-Isle, France) were acclimatized in the facility one week before to experiment start (Fig. 1). Mice had free access to water and chow. On the third day of acclimatization, Nutella (imported by Ferrero, Malmø, Sweden) was administered to ensure the mice were familiar with the treatment mode. From the following day until euthanasia, buprenorphine hydrochloride glucose monohydrate (Indivior Europe Limited, Dublin, Ireland) was supplemented to the Nutella (0.3 mg/g) and 125 mg Nutella/buprenorphine mix was provided per mouse. On day 0 of the experiment, the back of the mice was shaven (Aesculap electric shaver, Pennsylvania, USA), and the mice were covered with a protective plate and fire blanket (Viking, Esbjerg, Denmark) except for an exposed area of 1.5 × 1.5 cm between the scapular of the mouse. Full-thickness necrosis was created with a hot air gun (preheated) for 5 s at a fixed distance of 5 cm from the burner mouthpiece to the skin, as previously described [3]. The procedure was done in general anesthesia (250 μL Hypnorm - fentanyl citrate, 78.75 μg/ml; fluanisone, 2.5 mg/ml, Vetapharma Ltd, Leeds, UK, combined with midazolam - 1.25 mg/ml, Accord Healthcare AB, Solna, Sweden). Post-procedure, the mice were administered 1 mL saline s.c. and placed on heated electrical mats with cage enrichment toys, pre-watered chow, water, and Nutella containing buprenorphine easily accessible. Mice were active and showed no discomfort a few h after the procedure. On the fourth day, three alginate beads with *P. aeruginosa* were installed under the non-burned skin, and three beads were installed under the eschar. The beads were prepared fresh and kept refrigerated for 16 h prior to experiment start. On the day of the bead installation in the animals, control beads were blended and plated to assess the initial bacteriology and vitality of cells. The small surgical incision between the two segments was closed with a surgical stapler (Braintree Scientific Autoclip, Fisher Scientific).

3. Intervention

After 15 min, the mice were randomly assigned to the following three groups.

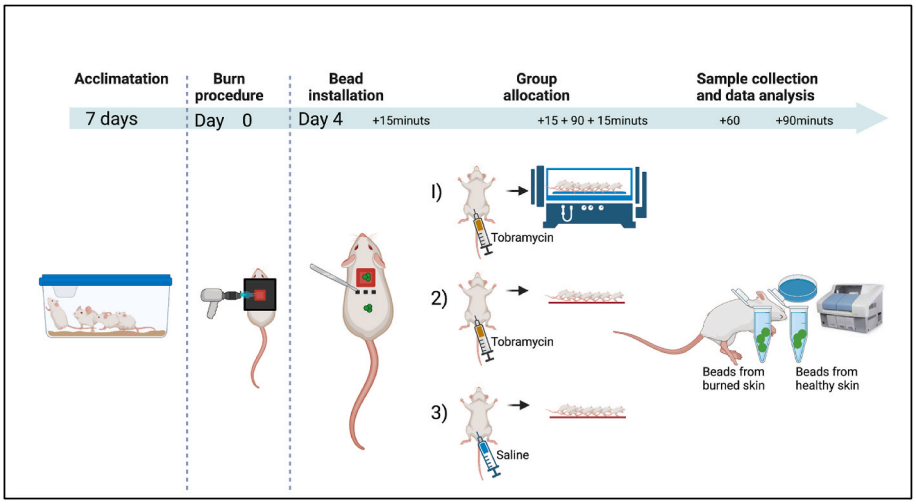

Fig. 1. Experimental setup. Mice were acclimatized for a week, followed by a full-thickness necrosis located mid-scapular. Four days after the burning procedure, an incision (0.5 cm) caudally from the wound was made. Three alginate beads containing P. aeruginosa were inserted through the incision and placed sub-eschar, and three beads were placed caudally for the incision. The lesion was clamped, securing the beads in allocated positions. Mice were anaesthetized and divided into three groups 1) Tobramycin and HBOT 2) Tobramycin 3) Saline. The injected liquids were given 15 min for distribution in the body, and the HBOT procedure was initiated. Mice not receiving HBOT were placed on heating mats during the procedure. Samples were collected after an additional 60 or 90 min.

1. Mice were administered tobramycin (0.8 mg/mouse, 0.2 mL s.c.). Dose determined from earlier publication [4]. Mice are placed on a heated mat for 15 min (37 °C) and then moved to the HBOT chamber (heated to 37 °C with a water system) for an additional 15 min of acclimatization to 2.8atm, followed by 90 min of treatment and 15 min of de-pressurization (Oxycom 250 ARC, Hypcom, Tampere, Finland) with 100% O2 and appropriate ventilation (n = 20).
2. Mice are administered tobramycin (0.8 mg/mouse, 0.2 mL sc) and placed on electrical heating mats during the procedure of group 1 (n = 20).
3. Placebo mice receiving saline were placed on electrical heating mats during the procedure of group 1 (n = 5).

All mice were under general anesthesia throughout the procedure.

Half of the number of mice from groups 1 and 2 were euthanized 3 h after receiving tobramycin and the remaining including the placebo group after 4.5 h (Fig. 2).

The experiment was replicated with 22 mice in the first round and 23 in the second. All results were pooled.

3.1. Alginate bead production

A 3% alginate solution was prepared by dissolving Protanal LF 10/60 (IMCD, Helsingør, Denmark) in 0.9% NaCl and sterilized by heating (95 °C for 15 min). *P. aeruginosa* was grown overnight in lysogeny broth and resuspended to optical density 0.3 (600 nm) before diluting the bacteria culture 1:20 in alginate.

A syringe with a flexible plastic tube filled with the solution was attached to a drip counter (Graseby 3100; Ardus Medical Inc., Watford, UK). The pump was running with a fixed flow rate of 40 mL/h. The *P. aeruginosa* alginate suspension formed spherical droplets when falling 8 cm into a gelling bath containing 0.1 M Tris – HCL and 12.5 mM $CaCl_2$. A magnetic stirrer (VWR lab disc, Rødovre, Denmark) was placed underneath the gelling bath to separate the beads. Once the stabilization process was finished (1 h), the beads were washed thrice in 0.9% NaCl containing 0.1 M $CaCl_2$. Beads were stored in 0.9% NaCl containing $CaCl_2$ to maintain stability. The mean diameter of the beads was 4.5 mm. The minimal inhibiting concentration (MIC) for tobramycin of the PAO1 strain used is 1.5 mg/L (Etest, bioMérieux, Marcy-l'Étoile, France).

3.2. Beads - Quantitative bacteriology

Beads from under the non-burned- and the burned skin were recovered from the subcutaneous installation *in toto*. The three beads from the non-burned skin were pooled into 2 mL microcentrifuge tubes (Nerbe plus, Winsen/Luhe, Germany), and the three beads from the burned skin were pooled into a similar tube. All tubes contained three glass beads and 1 mL citric acid buffer, pH 7. The alginate beads were homogenized (TissueLyser II; Qiagen, Copenhagen, Denmark) for 30 s at a frequency of 30/s. Subsequently, 0.85 mL PBS was added to stabilize the solution. The homogenates were serial diluted in saline, plated on solid lactose agar plates ('Blue plates) for gram negative rods. These plates consist of a modified Conradi-Drigalskimedium containing 10 g/L detergent, 1 g/L Na2S2O3•H2O, 0.1 g/L bromothymol blue, 9 g/L lactose and 0.4 g/L glucose, pH 8.0; produced at SSI. Plates were incubated overnight, and the CFU was counted the next day for quantitative bacteriology.

All homogenates were centrifuged at 5000 rpm for 15 min, and the supernatants were sterile filtered (0.22 μm) and frozen at −80 °C before tobramycin concentration measurements.

3.3. Beads - Tobramycin measurements

The total concentration of tobramycin in the alginate beads was measured using a Thermo Scientific Indiko (Clinical Diagnostics, Thermo Fisher Scientific, Allerød, Denmark). The range of the tobramycin assay is 0.0–10.0 μg/mL.

3.4. Statistical analysis

Statistical analysis of data was performed using GraphPad Software, Inc., La Jolla, CA, USA. Data are presented as medians ±95% confidence intervals. Differences between the groups were calculated with *Kruskal–Wallis* test. The level of significance was set to p = 0.05.

3.5. Ethics

The animal experiment complies with the ARRIVE guidelines and has an approval number (2020-15-0201-00535) from the *Animal Experiments Inspectorate* (AIRD).

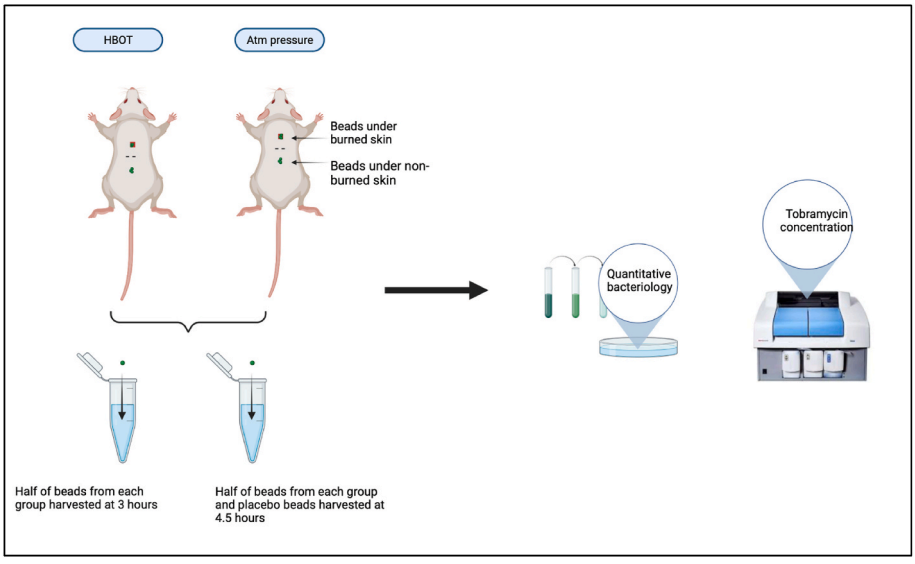

Fig. 2. Schematic drawing of mice with inserted beads allocated to either HBO or atmospheric treatment. Beads were collected after the procedure, lysed and plated for quantitative bacteriology, and analyzed for tobramycin concentration.

4. Results

4.1. Quantitative bacteriology

The quantitative bacteriology in the biofilm beads in the burned skin significantly decreased at 3 and 4.5 h adding HBOT ($p = 0.043$ and 0.0089) as compared to the atmospheric group (Fig. 3). The regrowth of the bacteria declined from 3 to 4.5 h when the mice were treated with HBOT.

The quantitative bacteriology was also decreased in the beads under the non-burned skin when HBOT was applied as compared to the non-HBOT group, but only at 4.5 h ($p = 0.015$). No significant reducing effect of the HBOT was seen at 3 h.

When comparing the quantitative bacteriology in biofilm beads under burned and non-burned skin, a difference was seen at 3 h ($p = 0.042$) with a higher CFU under the burned skin adding HBOT. No statistically significant difference was observed at 4.5 h.

The CFU level of all treatment groups was significantly reduced from the placebo group that received neither Tobramycin nor HBOT.

4.2. Tobramycin biofilm concentrations

The tobramycin contained in the beads was increased by HBOT when placed under the burned skin at both time points (at 3 h, $p = 0.031$, and 4.5 h, $p = 0.0078$) as compared to the atmospheric group (Fig. 4).

Tobramycin concentrations were not increased in the beads under non-burned tissue when HBOT was applied as compared to the atmospheric group at either time point.

No difference in tobramycin concentration was detected when comparing the beads under non-burned skin and burned skin, at atmospheric conditions at the 3-h time point. At 4.5 h, the highest tobramycin concentrations were revealed in beads under the burned skin in the HBOT group ($p = 0.006$).

No statistically significant changes in tobramycin concentration were identified during the 1.5 h between terminating time points in burn or non-burn groups and in either treatment arm.

5. Discussion

Understanding the dynamics between the invading pathogen, the host wound, the environment, and the antibiotic pharmacokinetics are essential for optimal treatment of chronic biofilm infected wounds. In the present study, we investigated the modification of a physiochemical component of the microenvironment by means of HBOT on the antibiotic pharmacokinetics/-dynamic (PK/PD) of tobramycin in a *P. aeruginosa* infected wound mice model. Using enlarged beads as a biofilm *by proxy* allows us to recover the biofilm *in toto* and evaluate the antibiotic concentration and bacterial content (simultaneous PK/PD) from the wound directly after supplementing with HBOT [2–4]. We did observe a significantly improved anti-biofilm effect of the burned wounds in the HBOT group as compared to the atmospheric group, by means of increased bacterial killing. In addition, this effect was paralleled by a significantly increased tobramycin concentration in the corresponding alginate beads.

The present study was performed using humanized HBOT conditions, directly translated from the conditions used to treat patients with HBO [18]. The adjunctive effect of HBOT can be attributed to increased O_2 pressure in the biofilm surrounding tissue and increased O_2 pressure in the alginate beads. The mechanism of the HBOT can be attributed to 1) an antibiotic potentiating effect 2) a direct O_2 mediated killing of the bacteria and 3) an immune stimulating effect of the host cells.

We found that HBOT ameliorated the biofilm compartment predisposition by increasing the penetration of tobramycin into the *P. aeruginosa* alginate beads under the burned skin and lowering the bacterial count. This anti-biofilm compartmentalizing effect was measurable after tobramycin administration followed by just one HBOT treatment of 90 min. These findings even persisted at least until 4.5 h. This suggests that the temporary effect of HBOT that counters the hypoxic conditions of the wound outlasts the treatment itself.

In normal tissue a transcutaneous oxygen tension ($TcPO_2$) of 30–50 mmHg has been reported, whereas $TcPO_2$ as low as 5–20 mmHg has been reported in ischemic pathological tissue [19]. However, during HBOT $TcPO_2$ can achieve levels above 200 mmHg, independently of the blood supply [20]. For our setup, this implies that the anti-biofilm effect of HBOT is expected to be significantly more pronounced in burned wounds with tissue necrosis as compared to the substantially less affected non-burned skin. Indeed, the anti-biofilm effect was significantly better in the beads under burned skin as compared to beads under non-burned skin.

The extra polysaccharide substance (EPS) and dead cells in the biofilm act like a permeability barrier and restricts diffusion into the matrix [21]. Our data support that an increased tobramycin penetrance is

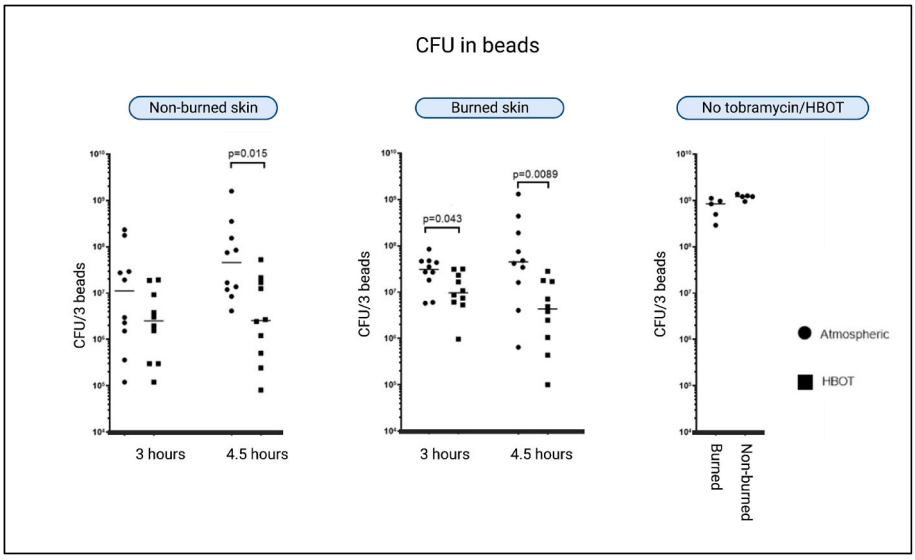

Fig. 3. Quantitative bacteriology (CFU/3 beads). Left panel: Beads collected from under non-burned skin at 3- and 4.5-h timepoint. Middle panel: Beads collected from under the burned skin at 3- and 4.5-h timepoint. Right panel: Beads collected from under-burned and non-burned skin at 4.5 h in mice receiving saline and atmospheric treatment.

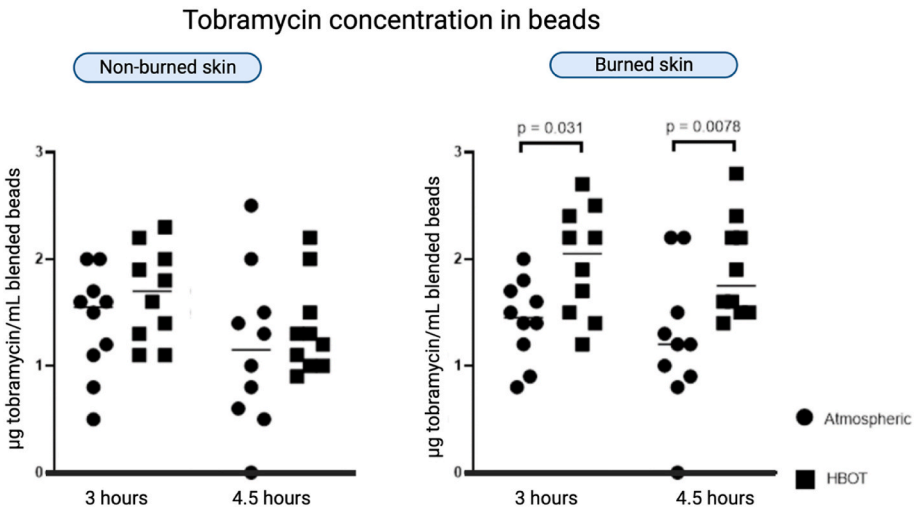

Fig. 4. Tobramycin measurements. The left panel displays beads collected from under non-burned skin in mice receiving either atmospheric or HBO treatment. No statistical differences between groups were detected. The right panel displays beads collected from under burned skin in mice receiving either atmospheric or HBO treatment. Higher tobramycin levels were detected in beads receiving HBOT compared to atmospherically treated mice.

achieved by correcting the burned tissue oxygenation with HBOT. Such effect could lead to boost of the phagocytosis and debris cleaning and facilitate the neutrophils' respiratory burst important for bacterial killing, and inhibits the anaerobic bacterial proliferation [15,22,23]. HBOT also stimulates collagen maturation and fibroblast proliferation [24]. The production of lactate by NADPH oxidase (NOX-2) in phagocytes, which activates transcription factors that support angiogenesis, also requires oxygen [25].

Chronic wounds are known to have an elevated alkaline environment compared to acute healing wounds, whereas alginate has a pH level of 3–3.5 [26,27]. *P. aeruginosa* is known to have increased biofilm-forming tendencies and antibiotic resistance development under acidic conditions. This behavior is thought to be reversible when returning to physiologically neutral conditions [28]. The efficacy of aminoglycosides has also been shown to depend on pH by being more efficient in alkaline surroundings [29]. This poses a risk of underestimating the effects of HBOT as a potentiating agent.

In a previous study using the same model as in the present study, tobramycin peaked in the alginate beads at around 3 h, followed by a protracted leakage from the beads over the next <20 h. Our results confirmed the 3–4.5 h tobramycin concentration drop from a previous work describing the first part of the concentration decline [4]. The significantly increased tobramycin concentrations observed in the alginate beads from the burned HBOT wounds as compared to the non-HBOT group was an unexpected observation. The effect was sustained during both evaluation time points, but which was on a 4-day distance to the thermal lesion. A direct effect, albeit unknown mechanism, of HBOT on both burned and non-burned skin at 3 h is indicated although the effect was not sustained at the 4.5 h timepoint in the non-burned skin only.

Concerning the specific antibacterial effect in the HBOT groups our study design did not allow for a clear distinction of the mechanisms. We evaluated the simultaneous antibiotic bead concentration and bacterial content (simultaneous biofilm microcompartment PK/PD). However, whether the actual increased anti-bacterial effect was due to increased bead concentration of tobramycin alone, or actual increased O_2 dependent bacterial tobramycin uptake or increased intra-bacterial accumulation of toxic hydroxyl radicals cannot be distinguished in the present study. However, the two latter mechanisms would benefit from the increased bead tobramycin concentration. The effect that persisted for 4.5 h was a direct HBOT killing or tobramycin potentiating effect resulting in a lower bacterial regrowth from 3 h to 4.5 h in the beads exposed to HBOT, regardless of skin condition. The tobramycin itself is known to induce the production of highly reactive free radicals, as is the HBOT, which promiscuously reacts and damaged intracellular components such as DNA, RNA, proteins, polysaccharides and phospholipids of *P. aeruginosa* [30]. This oxidative stress is also thought to contribute to changes in the metabolome [31]. The intrinsic susceptibility is influenced by this altered bacterial metabolic state, resulting in an even faster bactericidal action from tobramycin. HBOT has previously been shown to increase the antibiotic-killing efficiency in a PAO1 biofilm *in vitro* [32].

The anti-biofilm effect by applying HBOT may partly be explained by the possibility that HBOT accelerated bacterial growth by oxygenating the hypoxic biofilms and thus boost bacterial metabolism, which could lead to a more efficient tobramycin bacterial killing [31]. Strategies forcing biofilm living bacteria out their resting persister states into more metabolic active phenotypes and thereby rendering them increasingly susceptible to antibiotic therapy, has been argued [33,34]. However, our study setup did not allow to investigate these specific mechanisms of HBOT. Furthermore, the most pronounced anti-biofilm effect of HBOT was observed in situations where tobramycin was also significantly increased.

In contrast, we did find a bacterial count significantly higher in beads under burned skin than under non-burned skin at the 3 h timepoint, with no significant difference in corresponding tobramycin content, suggesting that the CFU level did not represent the antibiotic killing effect but could represent a direct intrinsic killing effect of HBOT complimenting the effects mediated by tobramycin.

5.1. Limitations

Biofilm formation is influenced by quorum sensing molecules like *N-butonoyl-L-homoserine lactone* (BHL) [35]. The effect of the HBOT on quorum sensing molecules was not investigated and an anti-quorum sensing effect cannot be ruled out. However, the present study did not aim at investigating biofilm formation, but tobramycin antibacterial enhancing HBOT effect.

The alginate bead model simulates a biofilm created *ex-situ* and inoculated in a living host. This mature biofilm has a phenotype that does not constitute the age-corresponding level of other important components like rhamnolipid, polysaccharide, and eDNA. It is known that antibiotic tolerance increases with the age of the biofilm and that eDNA plays a role in stabilizing the biofilm, which we also demonstrated earlier using this model (4). For this setup, though, the model makes it possible to examine the biofilm as a completely independent entity

regarding simultaneous tobramycin uptake and quantitative bacteriology.

6. Conclusion

The microenvironment of the *P. aeruginosa* biofilm depends on the fitness of the external environment. HBOT reoxygenates the wound bed and biofilm and acts as an anti-biofilm adjunct to tobramycin through lowered bacteriology, higher antibiotic penetration into the wound biofilm, and hindering the regrowth. Understanding the PK/PD nature of biofilms and identifying and later implementing anti-biofilm adjuncts for antibiotics represent a promising non-antibiotic strategy for combating recalcitrant biofilm infections.

CRediT authorship contribution statement

Anne Sofie Laulund: Conceptualization, Methodology, All authors participated in the conceptualization and methodology design, The animal experiment was performed, The statistics and figures were made, the data was interpreted, The first draft of the manuscript was made. **Franziska Angelika Schwartz:** Conceptualization, Methodology, All authors participated in the conceptualization and methodology design, The animal experiment was performed, the data was interpreted. **Niels Høiby:** Conceptualization, Methodology, All authors participated in the conceptualization and methodology design. **Kim Thomsen:** Conceptualization, Methodology, All authors participated in the conceptualization and methodology design. **Claus Moser:** Conceptualization, Methodology, All authors participated in the conceptualization and methodology design, the data was interpreted, All authors contributed equally to the final uploaded manuscript.

Declaration of competing interest

The authors of this manuscript declare that they have no competing interests that could influence the objective presentation, interpretation, or evaluation of the research findings presented in this scientific article. No financial, personal, or professional conflicts of interest exist that could impact the integrity or credibility of the research process, analysis, or conclusions. This study has been conducted with transparency and adherence to the highest standards of scientific rigor and ethical conduct.

On behalf of all authors and with kind regards.

Data availability

Data will be made available on request.

References

[1] Malone M, Bjarnsholt T, McBain AJ, James GA, Stoodley P, Leaper D, et al. The prevalence of biofilms in chronic wounds: a systematic review and meta-analysis of published data. J Wound Care 2017;26:20–5. https://doi.org/10.12968/jowc.2017.26.1.20.

[2] Cao B, Christophersen L, Thomsen K, Sønderholm M, Bjarnsholt T, Jensen PØ, et al. Antibiotic penetration and bacterial killing in a Pseudomonas aeruginosa biofilm model. J Antimicrob Chemother 2015;70:2057–63. https://doi.org/10.1093/jac/dkv058.

[3] Cao B, Christophersen L, Kolpen M, Jensen PØ, Sneppen K, Høiby N, et al. Diffusion retardation by binding of tobramycin in an alginate biofilm model. PLoS One 2016;11:e0153616. https://doi.org/10.1371/journal.pone.0153616.

[4] Christophersen L, Schwartz FA, Lerche CJ, Svanekjær T, Kragh KN, Laulund AS, et al. In vivo demonstration of Pseudomonas aeruginosa biofilms as independent pharmacological microcompartments. J Cyst Fibros 2020. https://doi.org/10.1016/j.jcf.2020.01.009.

[5] Moser C, Pedersen HT, Lerche CJ, Kolpen M, Line L, Thomsen K, et al. Biofilms and host response - helpful or harmful. APMIS 2017;125:320–38. https://doi.org/10.1111/apm.12674.

[6] Brauner A, Fridman O, Gefen O, Balaban NQ. Distinguishing between resistance, tolerance and persistence to antibiotic treatment. Nat Rev Microbiol 2016;14:320–30. https://doi.org/10.1038/nrmicro.2016.34.

[7] Kaldalu N, Hauryliuk V, Tenson T. Persisters—as elusive as ever. Appl Microbiol Biotechnol 2016;100:6545–53. https://doi.org/10.1007/s00253-016-7648-8.

[8] Wood TK. Strategies for combating persister cell and biofilm infections. Microb Biotechnol 2017;10:1054–6. https://doi.org/10.1111/1751-7915.12774.

[9] Ciofu O, Tolker-Nielsen T. Tolerance and resistance of Pseudomonas aeruginosa biofilms to antimicrobial agents—how P. aeruginosa can escape antibiotics. Front Microbiol 2019;10. https://doi.org/10.3389/fmicb.2019.00913.

[10] Jo J, Price-Whelan A, Dietrich LEP. Gradients and consequences of heterogeneity in biofilms. Nat Rev Microbiol 2022;20:593–607. https://doi.org/10.1038/s41579-022-00692-2.

[11] Goswami AG, Basu S, Banerjee T, Shukla VK. Biofilm and wound healing: from bench to bedside. Eur J Med Res 2023;28:157. https://doi.org/10.1186/s40001-023-01121-7.

[12] Hendrickson MD, Poyton RO. Crosstalk between nitric oxide and hypoxia-inducible factor signaling pathways: an update. RRBC 2015;5:147–61. https://doi.org/10.2147/RRBC.S58280.

[13] Gupta S, Mujawdiya P, Maheshwari G, Sagar S. Dynamic role of oxygen in wound healing: a microbial, immunological, and biochemical perspective. Arch Razi Inst 2022;77:513–23. https://doi.org/10.22092/ARI.2022.357230.2003.

[14] Yip WL. Influence of oxygen on wound healing. Int Wound J 2014;12:620–4. https://doi.org/10.1111/iwj.12324.

[15] Sen CK. Wound healing essentials: let there Be oxygen. Wound Repair Regen 2009;17:1–18. https://doi.org/10.1111/j.1524-475X.2008.00436.x.

[16] Sanford NE, Wilkinson JE, Nguyen H, Diaz G, Wolcott R. Efficacy of hyperbaric oxygen therapy in bacterial biofilm eradication. J Wound Care 2018;27:S20–8. https://doi.org/10.12968/jowc.2018.27.Sup1.S20.

[17] Borriello G, Richards L, Ehrlich GD, Stewart PS. Arginine or nitrate enhances antibiotic susceptibility of Pseudomonas aeruginosa in biofilms. Antimicrob Agents Chemother 2006;50:382–4. https://doi.org/10.1128/AAC.50.1.382-384.2006.

[18] Löndahl M, Katzman P, Nilsson A, Hammarlund C. Hyperbaric oxygen therapy facilitates healing of chronic foot ulcers in patients with diabetes. Diabetes Care 2010;33:998–1003. https://doi.org/10.2337/dc09-1754.

[19] Castilla DM, Liu Z-J, Velazquez OC. Oxygen: implications for wound healing. Adv Wound Care 2012;1:225–30. https://doi.org/10.1089/wound.2011.0319.

[20] Ercengiz A, Mutluoglu M. Hyperbaric transcutaneous oximetry. StatPearls, treasure island (FL). StatPearls Publishing; 2023.

[21] Ciofu O, Moser C, Jensen PØ, Høiby N. Tolerance and resistance of microbial biofilms. Nat Rev Microbiol 2022;20:621–35. https://doi.org/10.1038/s41579-022-00682-4.

[22] van der Goes A, Brouwer J, Hoekstra K, Roos D, van den Berg TK, Dijkstra CD. Reactive oxygen species are required for the phagocytosis of myelin by macrophages. J Neuroimmunol 1998;92:67–75. https://doi.org/10.1016/s0165-5728(98)00175-1.

[23] Leeper-Woodford SK, Mills JW. Phagocytosis and ATP levels in alveolar macrophages during acute hypoxia. Am J Respir Cell Mol Biol 1992;6:326–34. https://doi.org/10.1165/ajrcmb/6.3.326.

[24] Thackham JA, McElwain DLS, Long RJ. The use of hyperbaric oxygen therapy to treat chronic wounds: a review. Wound Repair Regen 2008;16:321–30. https://doi.org/10.1111/j.1524-475X.2008.00372.x.

[25] André-Lévigne D, Modarressi A, Pepper MS, Pittet-Cuénod B. Reactive oxygen species and NOX enzymes are emerging as key players in cutaneous wound repair. Int J Mol Sci 2017;18:2149. https://doi.org/10.3390/ijms18102149.

[26] Lee KY, Mooney DJ. Alginate: properties and biomedical applications. Prog Polym Sci 2012;37:106–26. https://doi.org/10.1016/j.progpolymsci.2011.06.003.

[27] Khan M, Philip L, Cheung G, Vadakepeedika S, Grasemann H, Sweezey N, et al. Regulating NETosis: increasing pH promotes NADPH oxidase-dependent NETosis. Front Med 2018;5. https://doi.org/10.3389/fmed.2018.00019.

[28] Lin Q, Pilewski JM, Di YP. Acidic microenvironment determines antibiotic susceptibility and biofilm formation of Pseudomonas aeruginosa. Front Microbiol 2021;12:747834. https://doi.org/10.3389/fmicb.2021.747834.

[29] Milman N, Dahlager J. THE pH-DEPENDENT INFLUENCE OF AMINOGLYCOSIDE ANTIBIOTICS ON IODOHIPPURATE ACCUMULATION IN RABBIT RENAL CORTICAL SLICES. J Antibiot 1978;31:1183–7. https://doi.org/10.7164/antibiotics.31.1183.

[30] Stokes JM, Lopatkin AJ, Lobritz MA, Collins JJ. Bacterial metabolism and antibiotic efficacy. Cell Metabol 2019;30:251–9. https://doi.org/10.1016/j.cmet.2019.06.009.

[31] Lobritz MA, Belenky P, Porter CBM, Gutierrez A, Yang JH, Schwarz EG, et al. Antibiotic efficacy is linked to bacterial cellular respiration. Proc Natl Acad Sci U S A 2015;112:8173–80. https://doi.org/10.1073/pnas.1509743112.

[32] Kolpen M, Mousavi N, Sams T, Bjarnsholt T, Ciofu O, Moser C, et al. Reinforcement of the bactericidal effect of ciprofloxacin on Pseudomonas aeruginosa biofilm by hyperbaric oxygen treatment. INT J ANTIMICROB AG 2016;47:163–7. https://doi.org/10.1016/j.ijantimicag.2015.12.005.

[33] Fang X, Allison KR. Resuscitation dynamics reveal persister partitioning after antibiotic treatment. Mol Syst Biol 2023;19:e11320. https://doi.org/10.15252/msb.202211320.

[34] Wilmaerts D, Windels EM, Verstraeten N, Michiels J. General mechanisms leading to persister formation and awakening. Trends Genet 2019;35:401–11. https://doi.org/10.1016/j.tig.2019.03.007.

[35] Tuon FF, Dantas LR, Suss PH, Tasca Ribeiro VS. Pathogenesis of the Pseudomonas aeruginosa biofilm: a review. Pathogens 2022;11:300. https://doi.org/10.3390/pathogens11030300.